Inorganic Chemistry

Article

pubs.acs.org/IC

Syntheses, Structures, and Electronic Properties of Ba_3FeUS_6 and Ba_3AgUS_6

Adel Mesbah,[†] Christos D. Malliakas,[†] Sébastien Lebègue,[‡] Amy A. Sarjeant,[†] Wojciech Stojko,[†] Lukasz A. Koscielski,[†] and James A. Ibers*[,†]

[†]Department of Chemistry, Northwestern University, 2145 Sheridan Road, Evanston, Illinois 60208-3113, United States

[‡]Laboratoire de Cristallographie, Résonance Magnétique, et Modélisations CRM2 (UMR UHP-CNRS 7036), Faculté des Sciences et Techniques, Université de Lorraine, BP 70239, Boulevard des Aiguillettes, 54506 Vandoeuvre-lès-Nancy Cedex, France

Supporting Information

ABSTRACT: The compounds Ba_3FeUS_6 and Ba_3AgUS_6 have been synthesized by the reactions of BaS, U, S, and M (= Fe or Ag) at 1223 K. These two isostructural compounds crystallize in the K_4CdCl_6 structure type in the trigonal system in space group D_{3d}^6–$R\bar{3}c$. Both structures feature infinite $^1_\infty[MUS_6^{6-}]$ chains along c that are separated by Ba atoms. The $^1_\infty[FeUS_6^{6-}]$ chains are formed by the face-sharing of US_6 trigonal prisms with FeS_6 octahedra; in contrast, the $^1_\infty[AgUS_6^{6-}]$ chains are formed by the face-sharing of US_6 octahedra with AgS_6 trigonal prisms. The Ba_3FeUS_6 compound charge balances with 3 Ba^{2+}, 1 Fe^{2+}, 1 U^{4+}, and 6 S^{2-}, whereas Ba_3AgUS_6 charge balances with 3 Ba^{2+}, 1 Ag^{1+}, 1 U^{5+}, and 6 S^{2-}. This structure offers a remarkable flexibility in terms of the oxidation state of the incorporated uranium depending on the oxidation state of the d-block metal. DFT calculations performed with the HSE functional have led to band gaps of 2.3 and 2.2 eV for Ba_3FeUS_6 and Ba_3AgUS_6, respectively. From resistivity measurements, the Arrhenius activation energies are 0.12(1) and 0.43(1) eV for Ba_3FeUS_6 and Ba_3AgUS_6, respectively.

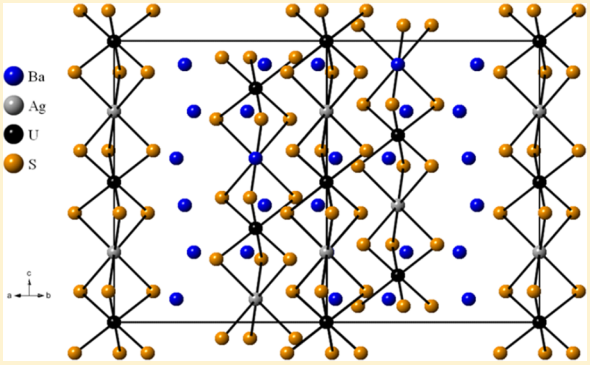

INTRODUCTION

The crystal chemistry of solid-state actinide chalcogenide compounds An/Q (An = Th, U, Np; Q = S, Se, Te) displays varied structural, electronic, magnetic, and optical properties.[1−3] Indeed, the 5f elements can adopt different formal oxidation states ranging from An^{3+} to An^{6+} that lead to the formation of new compounds. Among the An/Q compounds, An = U has been the most studied. These include U_2S_3,[4] PdU_2S_4,[5] $ScUS_3$,[5] and ScU_3S_6[6] [U^{3+}]; AUQ_6, $AMAnQ_3$, and MUQ_3 [U^{4+}];[1] and $Rb_4U_4P_4Se_{26}$,[7,8] $Tl_3Cu_4USe_6$,[9] and $K_2Cu_3US_5$[10] [U^{5+}]. Insofar as we know, there are no examples of purely U^{6+} in An/Q compounds. However, there are some mixed-valence compounds: $Ba_{3.69}US_6$,[11] $Ba_8Hg_3U_3S_{18}$,[12] [$U^{4+,5+}$]; and $A_6Cu_{12}U_2S_{15}$[13][$U^{5+,6+}$] (A = alkali metal; M = d-block element).

In the actinide chalcogenides Ak/An/Q (Ak = alkaline-earth metal), besides the $Ba_{3.69}US_6$[11] and $Ba_8Hg_3U_3S_{18}$[12] compounds mentioned above, the other reported structures Ba_2AnS_6,[14] $AkAn_2Q_5$,[11,15−17] $BaUS_3$,[11,18,19] $Ba_2Cu_2AnS_5$,[20,21] and $Ba_4Cr_2US_9$[22] contain only An^{4+}. In our continued exploration of the crystal chemistry of the Ak/U/S compounds, particular attention has been paid to the $Ba_{3.69}US_6$ structure, which crystallizes in the K_4CdCl_4[23] structure type. This structure is characterized by the presence of two crystallographic sites (symmetries 32 and $\bar{3}$), where U and the d-block metal may reside. These two sites provide an interesting flexibility that allows the tuning of the formal oxidation state of U. Here, we provide such an example in the new compounds Ba_3FeUS_6 and Ba_3AgUS_6, both of which crystallize in the K_4CdCl_4[23] structure type. We present their syntheses, structures, resistivities, and electronic structures.

EXPERIMENTAL METHODS

Caution! *Depleted U is an α-emitting radioisotope and, as such, is considered a health risk. Its use requires appropriate infrastructure and personnel trained in the handling of radioactive materials.*

Syntheses. The following reactants were used as obtained: BaS (Alfa, 99.7%), Ag (Aldrich, 99.99%), Fe (Aesar, 99.99%), Sb (Aldrich, 99.5%), and S (Mallinckrodt, 99.6%). U powder was obtained by the hybridization of depleted turnings (Oak Ridge National Laboratory) and decomposition of the resulting hydride in a modification[24] of a previous literature method.[25] Sb_2S_3, used as a flux, was obtained from the stoichiometric reaction of Sb and S at 1273 K for 24 h.

Reactions to synthesize Ba_3FeUS_6 and Ba_3AgUS_6 were performed in sealed carbon-coated fused-silica tubes (6 mm). The starting mixtures were loaded into tubes in a glovebox under an Ar atmosphere. The tubes were then removed from the drybox, evacuated to 10^{-4} Torr, flame-sealed, and placed in a computer-controlled furnace.

Synthesis of Ba_3FeUS_6. Black blocks of Ba_3FeUS_6 were obtained by direct combination of U (20 mg, 0.08 mmol), Fe (22 mg, 0.39

Received: October 23, 2013
Published: February 24, 2014

   dx.doi.org/10.1021/ic4026574 | Inorg. Chem. 2014, 53, 2899−2903

mmol), BaS (80 mg, 0.47 mmol), and S (22.5, 0.70 mmol). The reaction mixture was heated to 1223 K in 48 h, held at this temperature for 8 days, then cooled to 473 K at the rate of 3 K/h, and then the furnace was turned off. Black blocks were obtained in high yield. A few crystals were selected and analyzed with an EDX-equipped Hitachi S-3400 SEM. Two new quaternaries containing Ba:Fe:U:S were detected, one of which had the approximate molar ratio of 3:1:1:6. It was obtained in approximately 50 wt % yield, with the other products being the uncharacterized Ba/Fe/U/S quaternary and UOS.

Synthesis of Ba_3AgUS_6. This compound was synthesized by mixing U (30 mg, 0.13 mmol), Ag (13.5 mg, 0.13 mmol), BaS (63 mg, 0.37 mmol), S (12 mg, 0.37 mmol), and Sb_2S_3 (30 mg, 0.09 mmol) used as a flux. The reaction mixture was heated to 1223 K in 48 h, held there for 8 days, cooled to 673 K at the rate of 3 K/h, and then cooled to 293 K at the rate of 50 K/h. In addition to black columnar crystals of Sb_2S_3, black blocks of Ba_3AgUS_6 were obtained in low yield. The same reaction was repeated without Sb_2S_3 and led to the formation of smaller black blocks of Ba_3AgUS_6 in approximately 80 wt % yield. EDX analyses showed the presence of Ba:Ag:U:S in a ratio of 3:1:1:6. Byproducts were UOS and BaS.

Structure Determinations. Single-crystal X-ray diffraction data for Ba_3FeUS_6 and Ba_3AgUS_6 were collected with the use of graphite-monochromatized Mo Kα radiation (λ = 0.71073 Å) at 100(2) K on a Bruker APEX2 difractometer. The data collection strategy consisting of a series of 0.3° scans in ω and φ was optimized through the algorithm COSMO in the program APEX2.[26] The crystal-to-detector distance was 6 cm. The exposure times of 5 and 10 s/frame were used for Ba_3FeUS_6 and Ba_3AgUS_6, respectively. Data collection, cell refinement, and data reduction were carried out with the use of the program APEX2.[26] Face-indexed absorption, incident beam, and decay corrections were performed by the mean of the program SADABS.[27] Both structures were solved and refined with the shelx-13 algorithms of the SHELXTL package.[27,28] The refinement of the Ba_3AgUS_6 structure was straightforward, whereas that of Ba_3FeUS_6 involved the refinement of an obverse/reverse twin (twin component 0.104(2)). Crystal structure and refinement details are given in Table 1 and in the Supporting Information.

Table 1. Crystal Data and Structure Refinements for Ba_3FeUS_6 and Ba_3AgUS_6[a]

	Ba_3FeUS_6	Ba_3AgUS_6
fw (g mol^{-1})	898.26	950.28
a (Å)	12.0314(4)	12.1630(3)
c (Å)	13.3812(5)	13.9400(4)
V (Å^3)	1677.5(1)	1786.0(1)
ρ (g cm^{-3})	5.335	5.301
μ (mm^{-1})	27.159	25.936
$R(F)^b$	0.0210	0.0132
$R_w(F_o^2)^c$	0.0558	0.0276

[a]For both compounds: space group D_{3d}^6–$R\bar{3}c$, Z = 6, λ = 0.71073 Å, T = 100(2) K. [b]$R(F) = \sum||F_o| - |F_c||/\sum|F_o|$ for $F_o^2 > 2\sigma(F_o^2)$. [c]$R_w(F_o^2) = \{\sum w(F_o^2 - F_c^2)^2/\sum wF_o^4\}^{1/2}$. For $F_o^2 < 0$, $w^{-1} = \sigma^2(F_o^2)$; for $F_o^2 \geq 0$, $w^{-1} = \sigma^2(F_o^2) + (qF_o^2)^2$, where q = 0.0 for Ba_3FeUS_6 and 0.0043 for Ba_3AgUS_6.

Resistivity Measurements. Two-probe temperature-dependent resistivity data were collected with a homemade resistivity apparatus equipped with a Keithley 617 electrometer and a high-temperature vacuum chamber controlled by a K-20 MMR system. Data acquisition was controlled by custom-written software. Graphite paint (PELCO isopropanol-based graphite paint) was used to secure electrical contacts on the sample with copper wire of 0.025 mm in thickness (Omega). The direct current was applied along an arbitrary direction. Measurements were made on single crystals with dimensions of 0.095 × 0.097 × 0.015 mm for Ba_3FeUS_6 and 0.534 × 0.762 × 0.251 mm for Ba_3AgUS_6.

Ab Initio Calculations. The ab initio calculations were performed with density functional theory.[29] The Vienna Ab initio Simulation Package (VASP),[30,31] implementing the projector-augmented wave method,[32] was used with the default cutoff for the plane-wave part of the wave function and a 4 × 4 × 4 mesh to integrate over the Brillouin zone. Structural relaxations were performed with the generalized gradient approximation[33] (GGA) for the exchange-correlation potential, while the Heyd, Scuseria, and Ernzerhof (HSE06)[34−36] functional was used to obtain realistic values of the band gaps. The experimental geometries, converted to the VASP format with the CIF2Cell software,[37] served as the starting point for the relaxation process using the GGA functional. However, for the HSE calculations, the structural parameters were kept at their experimental values. Spin polarization was allowed in all calculations. The ground-state magnetic order was found by exploring all the possible magnetic orders in the crystallographic cell, the one with the lowest total energy being the ground state.

RESULTS

Syntheses. Black blocks of Ba_3FeUS_6 were obtained by direct combination of BaS, U, Fe, and S at 1223 K. The approximate yield was 50 wt % based on U content. Byproducts were another Ba/Fe/U/S quaternary and UOS. The compound Ba_3AgUS_6 was obtained first in low yield at 1123 K with Sb_2S_3 as a flux and then in high yield (≈80 wt %) by direct combination at 1223 K.

Structures. The compounds Ba_3FeUS_6 and Ba_3AgUS_6 are isostructural and crystallize in the K_4CdCl_6[23] structure type. They each contain six formula units in the trigonal space group D_{3d}^6–$R\bar{3}c$, with a = 12.0314(4) Å, c = 13.3812(5) Å for Ba_3FeUS_6 and a = 12.1630(3) Å, c = 13.9400(4) Å for Ba_3AgUS_6. Selected interatomic distances are given in Table 2.

Table 2. Selected Interatomic Distances (Å) in Ba_3FeUS_6, Ba_3AgUS_6, and $Ba_{3.69}US_6$[a]

distance[b]	Ba_3FeUS_6	Ba_3AgUS_6	$Ba_{3.69}US_6$[c]
U–S × 6	2.712(1)[d]	2.609(1)[e]	2.658(1)[e]
M–S × 6	2.554(1)[e]	2.880(1)[d]	3.079(1)[d,f]
Ba–S ×2	3.141(1)	3.149(1)	3.218(1)
	3.175(1)	3.192(1)	3.240(1)
	3.273(1)	3.303(1)	3.280(1)
	3.305(1)	3.385(1)	3.404(1)

[a]All three compounds crystallize in the K_4CdCl_6 structure type. [b]To facilitate comparisons within the text and in this table, distances have been rounded to three significant figures. [c]Reference 11. [d]Symmetry site 32. [e]Symmetry site $\bar{3}$. [f]M = Ba_2; occupancy = 0.69.

Ba_3FeUS_6. The asymmetric unit contains one U atom (site symmetry 32), one Fe atom ($\bar{3}$.), one Ba atom (.2), and one S atom (1). A general view of the structure along the [110] direction is shown in Figure 1. Each U atom is at the center of a trigonal prism of six S atoms (U–S = 2.712(1) Å). Each Fe atom is octahedrally coordinated by six S atoms (Fe–S = 2.554(1) Å). In the structure, US_6 trigonal prisms and FeS_6 octahedra share triangular faces to form chains along the c axis (Figure 1); Ba atoms are positioned between the chains as viewed in Figure 2. Each Ba atom is surrounded by eight S atoms.

Ba_3AgUS_6. This compound has the same structure as Ba_3FeUS_6 except that the positions of U and Ag are reversed with the U atom having site symmetry ($\bar{3}$.) and the Ag atom having site symmetry 32. As a result, each U atom is octahedrally coordinated by six S atoms (U–S = 2.609(1) Å) and each Ag is trigonal-prismatically coordinated by six S atoms

dx.doi.org/10.1021/ic4026574 | Inorg. Chem. 2014, 53, 2899−2903

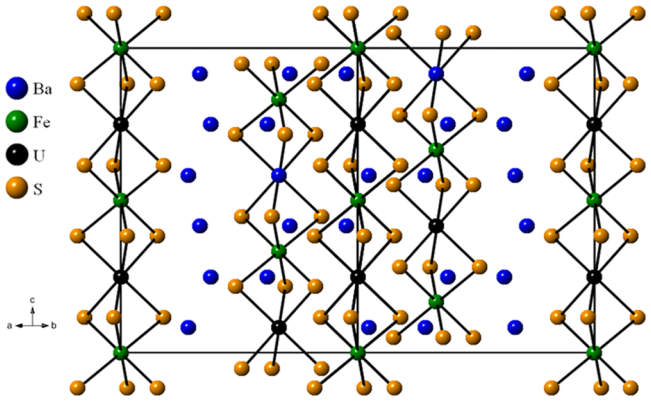

Figure 1. General view of the structure of Ba_3FeUS_6 down [110].

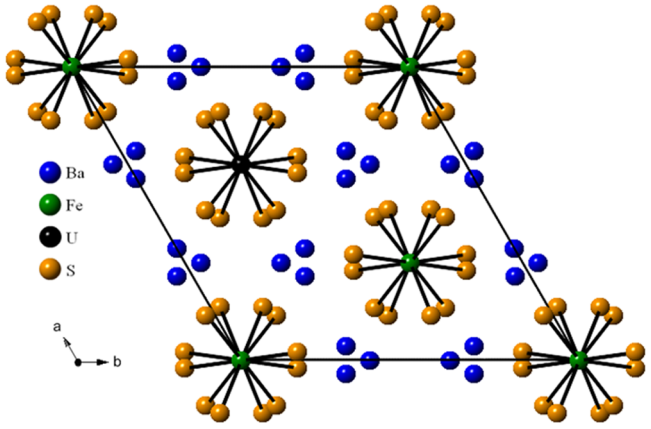

Figure 2. General view of the structure of Ba_3FeUS_6 down the *c* axis.

(Ag−S = 2.880(1) Å). In the structure, US_6 octahedra and AgS_6 trigonal prisms share triangular faces to form chains along the *c* axis (Figure 3); Ba atoms are positioned between the chains as viewed in Figure 4. Figure 5 presents a comparison of the chains in these two structures.

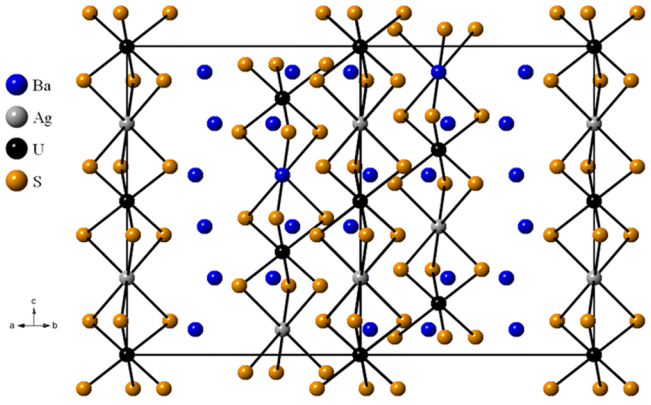

Figure 3. General view of the structure of Ba_3AgUS_6 down [110].

Formal Oxidation States. Table 2 provides selected interatomic distances found in the structures of Ba_3FeUS_6 and Ba_3AgUS_6 as well as those in the structure of $Ba_{3.69}US_6$.[11] In none of these structure are there significant S−S interactions. In the Ba_3UFeS_6, the Fe−S distance of 2.554(1) Å is the same as that of 2.552(1) Å in $FeUS_3$,[38] a compound containing six-coordinate Fe^{2+}. The U−S distance of

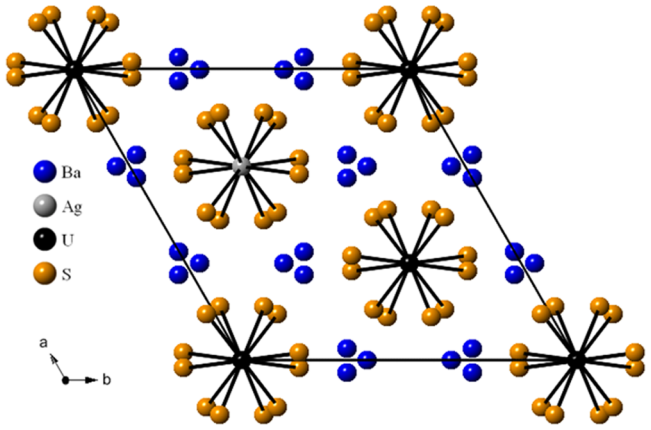

Figure 4. General view of the structure of Ba_3AgUS_6 down the *c* axis.

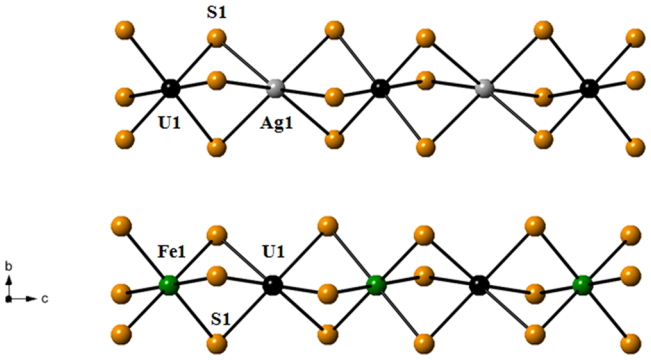

Figure 5. Comparison of $^1_\infty[MUS_6^{6-}]$ (M = Fe or Ag) chains in Ba_3FeUS_6 (top) and Ba_3AgUS_6 (bottom).

2.712(1) Å in Ba_3UFeS_6 is typical of six-coordinate U^{4+}, as found, for example, in $BaUS_3$ (2.668(1)−2.696(1)Å)[11] and $Ba_2Cu_2US_5$ (2.673(2)−2.770(1)Å).[21] Thus, the formal oxidation states in Ba_3FeUS_6 may be assigned as Ba^{2+}, Fe^{2+}, U^{4+}, and S^{2-}.

The U−S distance in Ba_3AgUS_6 of 2.609(1) Å is significantly shorter than those of six-coordinate U^{4+} in Ba_3UFeS_6 (2.712(1) Å) and the mixed six-coordinate $U^{4+,5+}$ of 2.658(1) Å in $Ba_{3.69}US_6$. The U−S distance compares well with the short distances found in $K_2Cu_3US_5$[10] (2 × 2.587(1) Å; 4 × 2.683(1) Å), a compound of U^{5+}. Table 3 provides a more extensive tabulation of U−S distances in related compounds.

Table 3. U−S Interatomic Distances in US_6 Polyhedra and Corresponding Oxidation States

compound	U oxidation state	U−S range (Å)[a]	reference
$BaUS_3$	+4	2.698(1)−2.696(1)	11
$Ba_2Cu_2US_5$	+4	2.673(2)−2.770(1)	21
Ba_3FeUS_6	+4	2.715(1)	this work
$Ba_8Hg_3U_3S_{18}$	mixed +4/+5	2.571(4)−2.743(3)	12
		2.595(4)−2.758(3)	
		2.602(4)−2.745(3)	
$Ba_{3.69}US_6$	mixed +4/+5	2.658(1)	11
Ba_3AgUS_6	+5	2.609(1)	this work
$K_2Cu_3US_5$	+5	2.587(1)−2.683(1)	10
$Cs_6Cu_{12}U_2S_{15}$	mixed +5/+6	2.598(2)	13

[a]To facilitate comparisons in this table, distances from the original CIF files, where necessary, have been rounded to three significant figures.

dx.doi.org/10.1021/ic4026574 | Inorg. Chem. 2014, 53, 2899−2903

Six-coordinate trigonal-prismatic Ag^{1+} is found in some oxides, for example, in $AgHg_3SbO_6$,[39] which also crystallizes in the K_4CdCl_6 structure type. However, insofar as we can determine, there are no examples of trigonal-prismatic AgS_6 for comparison with the current Ag−S distance of 2.880(1) Å, yet there are examples of octahedral AgS_6 for comparison: $Ag_{3.8}Sn_3S_8$, 2.855(1) Å;[40] $AgBi_2S_3Cl$, 2.722(2)−2.817(1) Å;[41] $ScAgP_2S_6$, 2.793(1) Å.[42] Thus, the formal oxidation states in Ba_3AgUS_6 may be assigned as Ba^{2+}, Ag^{1+}, U^{5+}, and S^{2-}.

Resistivity Behavior. The resistivity of a single crystal of Ba_3FeUS_6 decreases from 1.4 kΩ·cm at 300 K to 0.15 kΩ·cm at 500 K (Figure 6), consistent with semiconducting behavior.

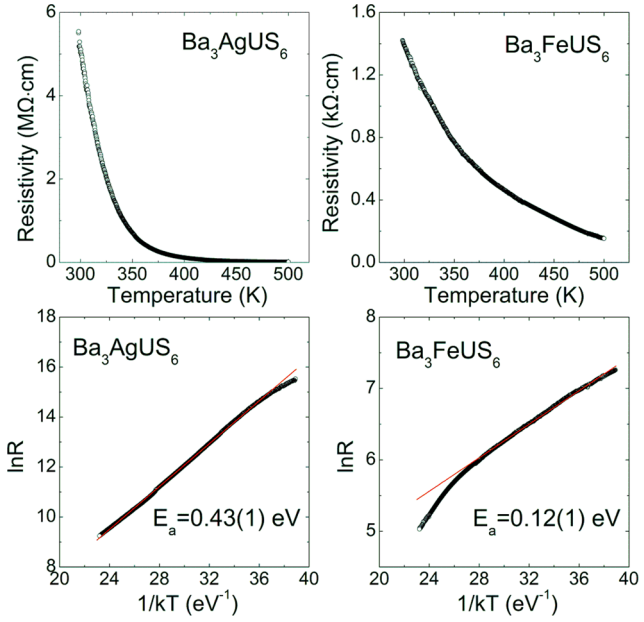

Figure 6. Resistivities and their corresponding Arrhenius plots for single crystals of Ba_3AgUS_6 and Ba_3FeUS_6.

The calculated Arrhenius activation energy is 0.12(1) eV. In the Arrhenius plot, a small deviation from linearity observed in the temperature range of 430−500 K is not consistent with a variable range hopping mechanism (Supporting Information). Rather, it may indicate a more complex carrier excitation mechanism at temperatures above 430 K. The resistivity of a single crystal of Ba_3AgUS_6 decreases from 5.5 MΩ·cm at 300 K to 10 kΩ·cm at 500 K, again consistent with semiconducting behavior. The calculated Arrhenius activation energy is 0.43(1) eV.

Electronic Properties. The ground states were first examined. For Ba_3FeUS_6, the ground-state magnetic order corresponds to an antiferromagnetic arrangement of the magnetic moments on the U atoms together with an antiferromagnetic arrangement of the magnetic moments on the Fe atoms. For Ba_3AgUS_6, the ground state is a ferromagnetic arrangement of the magnetic moments on the U atoms. The results of complete structural relaxation (atom positions, shape, and volume of the unit cell) for each system led to U−S = 2.69 Å, Fe−S = 2.50 Å, and Ba−S between 3.18 and 3.34 Å for Ba_3FeUS_6, and U−S = 2.62 Å, Ag−S = 2.89 Å, and Ba−S between 3.19 and 3.43 Å for Ba_3AgUS_6, in good agreement with the experimental values (Table 2). The small differences between theory and experiment may be attributed to intrinsic limitations of the GGA functional that was used, and to the effect of temperature. Figures 7 and 8 display the total and partial density of states (PDOS) for Ba_3FeUS_6 and

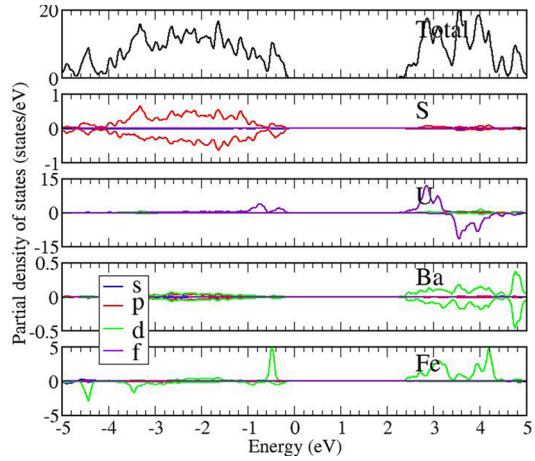

Figure 7. Total (upper plot) and partial density of states (lower plots) of Ba_3FeUS_6. For each atom, the PDOS is projected onto the relevant orbitals.

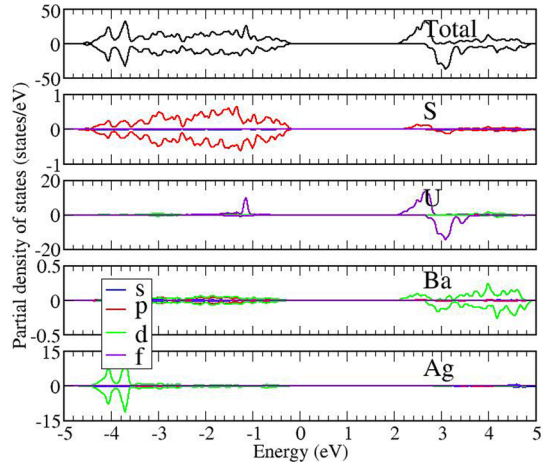

Figure 8. Total (upper plot) and partial density of states (lower plots) of Ba_3AgUS_6. For each atom, the PDOS is projected onto the relevant orbitals.

Ba_3AgUS_6, respectively, as computed using the HSE functional. The Fermi level is put at zero. We observe that Ba_3FeUS_6 is an insulator with a band gap of 2.3 eV. The spin polarization of the U and Fe species is clearly seen and induces a small magnetic moment on the S and Ba atoms. The top of the valence band and the bottom of the conduction band are derived mainly from U-f and Fe-d states, albeit with a small contribution from the S and Ba species. The total density of states (upper plot, Figure 7) shows no spin polarization because the compound is found to be an antiferromagnet. For Ba_3AgUS_6, which we found to be insulating, the band gap is 2.2 eV, slightly smaller than that for Ba_3FeUS_6. Because Ba_3AgUS_6 has a ferromagnetic ground state, the total density of states is polarized. This polarization, which comes mainly from the U atoms, induces a small spin polarization on the S and Ba species, but not on the Ag atoms. The top of the valence band corresponds to S-p and Ba-d states, whereas the bottom of the conduction band is mainly derived from U-f states.

dx.doi.org/10.1021/ic4026574 | Inorg. Chem. 2014, 53, 2899−2903

CONCLUSIONS

Two new quaternary solid-state uranium sulfides, namely, Ba_3FeUS_6 and Ba_3AgUS_6, were synthesized at 1223 K. These isostructural compounds crystallize in the K_4CdCl_6 structure type in the trigonal space group D_{3d}^6–$R\bar{3}c$. Their structure consists of infinite $^1_\infty[MUS_6^{6-}]$ (M = Fe or Ag) chains along the *c* axis separated by Ba atoms. The $^1_\infty[FeUS_6^{6-}]$ chains are formed by the face-sharing of US_6 trigonal prisms with FeS_6 octahedra; in contrast, the $^1_\infty[AgUS_6^{6-}]$ chains are formed by the face-sharing of US_6 octahedra with AgS_6 trigonal prisms. This structure offers a remarkable flexibility in terms of the oxidation state of the incorporated uranium depending on the oxidation state of the d-block metal. Thus, the Ba_3FeUS_6 compound charge balances with 3 Ba^{2+}, 1 Fe^{2+}, 1 U^{4+}, and 6 S^{2-}, whereas the Ba_3AgUS_6 compound charge balances with 3 Ba^{2+}, 1 Ag^{1+}, 1 U^{5+}, and 6 S^{2-}. Both compounds are semiconductors with calculated band gaps and measured Arrhenius activation energies of 2.3 and 0.12 eV for Ba_3FeUS_6 and 2.2 and 0.43 eV for Ba_3AgUS_6, respectively.

ASSOCIATED CONTENT

Supporting Information

Crystallographic files in CIF format for Ba_3FeUS_6 and Ba_3AgUS_6. For Ba_3FeUS_6, further discussion of the resistivity results. This material is available free of charge via the Internet at http://pubs.acs.org.

AUTHOR INFORMATION

Corresponding Author

*E-mail: ibers@chem.northwestern.edu.

Notes

The authors declare no competing financial interest.

ACKNOWLEDGMENTS

This research was kindly supported at Northwestern University by the U.S. Department of Energy, Basic Energy Sciences, Chemical Sciences, Biosciences, and Geosciences Division and Division of Materials Science and Engineering Grant ER-15522. Use was made of the IMSERC X-ray Facility at Northwestern University, supported by the International Institute of Nanotechnology (IIN). S.L. acknowledges HPC resources from GENCI-CCRT/CINES (Grant x2014-085106).

REFERENCES

(1) Bugaris, D. E.; Ibers, J. A. *Dalton Trans.* **2010**, *39*, 5949–5964.
(2) Narducci, A. A.; Ibers, J. A. *Chem. Mater.* **1998**, *10*, 2811–2823.
(3) Manos, E.; Kanatzidis, M. G.; Ibers, J. A. In *The Chemistry of the Actinide and Transactinide Elements*, 4th ed.; Morss, L. R., Edelstein, N. M., Fuger, J., Eds.; Springer: Dordrecht, The Netherlands, 2010; Vol. 6, pp 4005–4078.
(4) Zachariasen, W. H. *Acta Crystallogr.* **1949**, *2*, 291–296.
(5) Daoudi, A.; Noël, H. *J. Less-Common Met.* **1986**, *115*, 253–259.
(6) Julien, R.; Rodier, N.; Tien, V. *Acta Crystallogr., Sect. B: Struct. Crystallogr. Cryst. Chem.* **1978**, *34*, 2612–2614.
(7) Briggs Piccoli, P. M.; Abney, K. D.; Schoonover, J. D.; Dorhout, P. K. *Inorg. Chem.* **2001**, *40*, 4871–4875.
(8) Chondroudis, K.; Kanatzidis, M. G. *J. Am. Chem. Soc.* **1997**, *119*, 2574–2575.
(9) Bugaris, D. E.; Choi, E. S.; Copping, R.; Glans, P.-A.; Minasian, S. G.; Tyliszczak, T.; Kozimor, S. A.; Shuh, D. K.; Ibers, J. A. *Inorg. Chem.* **2011**, *50*, 6656–6666.
(10) Gray, D. L.; Backus, L. A.; Krug von Nidda, H.-A.; Skanthakumar, S.; Loidl, A.; Soderholm, L.; Ibers, J. A. *Inorg. Chem.* **2007**, *46*, 6992–6996.
(11) Mesbah, A.; Ibers, J. A. *J. Solid State Chem.* **2013**, *199*, 253–257.
(12) Bugaris, D. E.; Ibers, J. A. *Inorg. Chem.* **2012**, *51*, 661–666.
(13) Malliakas, C. D.; Yao, J.; Wells, D. M.; Jin, G. B.; Skanthakumar, S.; Choi, E. S.; Balasubramanian, M.; Soderholm, L.; Ellis, D. E.; Kanatzidis, M. G.; Ibers, J. A. *Inorg. Chem.* **2012**, *51*, 6153–6163.
(14) Mesbah, A.; Ringe, E.; Lebègue, S.; Van Duyne, R. P.; Ibers, J. A. *Inorg. Chem.* **2012**, *51*, 13390–13395.
(15) Narducci, A. A.; Ibers, J. A. *Inorg. Chem.* **1998**, *37*, 3798–3801.
(16) Brochu, R.; Padiou, J.; Prigent, J. *C. R. Acad. Sci. Paris* **1970**, *270*, 809–810.
(17) Brochu, R.; Padiou, J.; Prigent, J. *C. R. Seances Acad. Sci., Ser. C* **1972**, *274*, 959–961.
(18) Brochu, R.; Padiou, J.; Grandjean, D. *C. R. Seances Acad. Sci., Ser. C* **1970**, *271*, 642–643.
(19) Lelieveld, R.; IJdo, D. J. W. *Acta Crystallogr., Sect. B: Struct. Crystallogr. Cryst. Chem.* **1980**, *36*, 2223–2226.
(20) Mesbah, A.; Lebegue., S.; Klingsporn, J. M.; Stojko, W.; Van Duyne, R. P.; Ibers, J. A. *J. Solid State Chem.* **2013**, *200*, 349–353.
(21) Zeng, H.-y.; Yao, J.; Ibers, J. A. *J. Solid State Chem.* **2008**, *181*, 552–555.
(22) Yao, J.; Ibers, J. A. *Z. Anorg. Allg. Chem.* **2008**, *634*, 1645–1647.
(23) Beck, H. P.; Milius, W. *Z. Anorg. Allg. Chem.* **1986**, *539*, 7–17.
(24) Bugaris, D. E.; Ibers, J. A. *J. Solid State Chem.* **2008**, *181*, 3189–3193.
(25) Haneveld, A. J. K.; Jellinek, F. *J. Less-Common Met.* **1969**, *18*, 123–129.
(26) *Bruker APEX2 Version 2009.5-1: Data Collection and Processing Software*; Bruker Analytical X-Ray Instruments, Inc.: Madison, WI, 2009.
(27) Sheldrick, G. M. Department of Structural Chemistry, University of Göttingen: Göttingen, Germany, 2008.
(28) Sheldrick, G. M. *Acta Crystallogr., Sect. A: Found. Crystallogr.* **2008**, *64*, 112–122.
(29) Hohenberg, P.; Kohn, W. *Phys. Rev.* **1964**, *136*, 864–871.
(30) Schleid, T.; Meyer, G.; Morss, L. R. *J. Less-Common Met.* **1987**, *132*, 69–77.
(31) Kresse, G.; Joubert, D. *Phys. Rev. B* **1999**, *59*, 1758–1775.
(32) Blöchl, P. E. *Phys. Rev. B* **1994**, *50*, 17953–17979.
(33) Perdew, J. P.; Burke, K.; Ernzerhof, M. *Phys. Rev. Lett.* **1996**, *77*, 3865–3868.
(34) Heyd, J.; Scuseria, G. E.; Ernzerhof, M. *J. Phys. Chem.* **2003**, *118*, 8207–8215.
(35) Heyd, J.; Scuseria, G. E.; Ernzerhot, M. *J. Chem. Phys.* **2006**, *124*, 219906.
(36) Paier, J.; Marsman, M.; Hummer, K.; Kresse, G.; Gerber, I. C.; Angyan, J. G. *J. Chem. Phys.* **2006**, *125*, 249901.
(37) Björkman, T. *Comput. Phys. Commun.* **2011**, *182*, 1183–1186.
(38) Jin, G. B.; Ringe, E.; Long, G. J.; Grandjean, F.; Sougrati, M. T.; Choi, E. S.; Wells, D. M.; Balasubramanian, M.; Ibers, J. A. *Inorg. Chem.* **2010**, *49*, 10455–10467.
(39) Klein, W.; Jansen, M. *Acta Crystallogr., Sect. C: Cryst. Struct. Commun.* **2005**, *C61*, i94–i95.
(40) Amiel, O.; Frankel, D. C.; Wada, H. *J. Solid State Chem.* **1994**, *116*, 409–421.
(41) Ruck, M.; Schmidt, P. *Z. Anorg. Allg. Chem.* **2003**, *629*, 2133–2143.
(42) Lee, S.; Colombet, P.; Ouvrard, G.; Brec, R. *Inorg. Chem.* **1987**, *27*, 1291–1294.